

Antitumor Agents. 3. Design, Synthesis, and Biological Evaluation of New Pyridoisoquinolindione and Dihydrothienoquinolindione Derivatives with Potent Cytotoxic Activity

Adele Bolognese,^{*,†} Gaetano Correale,[†] Michele Manfra,[†] Antonio Lavecchia,[§] Orazio Mazzoni,[§] Ettore Novellino,[§] Paolo La Colla,[‡] Giuseppina Sanna,[‡] and Roberta Loddo[‡]

Dipartimento di Chimica Organica e Biochimica, Università di Napoli "Federico II", Via Cynthia 6, Monte Sant'Angelo, I-80126 Napoli, Italy, Dipartimento di Chimica Farmaceutica e Tossicologica, Università di Napoli "Federico II", Via D. Montesano 49, I-80131 Napoli, Italy, and Dipartimento di Biologia Sperimentale, Sezione di Microbiologia, Università di Cagliari, Cittadella Universitaria SS 554, I-09042 Monserrato, Cagliari, Italy

Received June 6, 2003

New antiproliferative compounds, the 1-aryl-3-ethoxycarbonyl-pyrido[2,3-*g*]isoquinolin-5,10-diones (PIQDs, **1–7**), were designed on the basis of a molecular model obtained by aligning the common quinolinquinone substructure of 5*H*-pyrido[3,2-*a*]phenoxazin-5-one (PPH) and some known anticancer agents. A Diels–Alder reaction between quinolin-5,8-dione (QD) and a 2-azadiene, formed by demolition of 2-aryl-1,3-thiazolidine ethyl esters (**T** compounds), was used to produce **1–7** and the isomeric 1-aryl-3-ethoxycarbonylpyrido[3,2-*g*]isoquinolin-5,10-diones (**8–14**). Two other compounds, the 3-amino-3-ethoxycarbonyldihydrothieno[2,3-*g*]quinolin-4,9-dione (**15**) and the 3-amino-3-ethoxycarbonyldihydrothieno[3,2-*g*]quinolin-4,9-dione (**16**), arising from a 1,4 Michael reaction of QD with a thiolate species formed by opening of **T** compounds, were recovered from the reaction mixture. The antiproliferative activity of **1–16** was evaluated against representative human liquid and solid neoplastic cell lines. The IC₅₀ of these compounds had median values in the range 2.00–0.01 μM, with **2–4** and **15** exhibiting significantly higher in vitro cytotoxic activity. Compound **2**, also evaluated against KB subclones (KB^{MDR}, KB^{7D}, and KB^{V20C}), was shown to be scarcely subject to the MDR1/P-glycoprotein drug efflux pump responsible for drug resistance. The noncovalent DNA-binding properties of PIQDs were examined using UV–vis and ¹H NMR spectroscopy experiments. Accordingly, these compounds were confirmed to have an ability to intercalate into double-stranded DNA by topoisomerase I superhelix unwinding assay. Interesting structure–activity relationships were found. Three important features seem to contribute to the cytotoxic activity of these anticancer ligands: (i) the DNA intercalating capability of the three-cyclic quinonic system, typical of this class of compounds, (ii) the position of the pendant phenyl ring that, according to the superimposition model, must occupy the same area of the corresponding benzo-fused ring A of PPH, and (iii) the effect of electron-withdrawing substituents on the phenyl ring, which can contribute improving the π–π stacking interactions between ligand and DNA base pairs. Besides, a mechanism of action suspected to involve topoisomerases could be hypothesized to interpret the antiproliferative activity of the thienoquinolindione **15**, which can be regarded as a cyclic cysteine derivative.

Introduction

Quinone derivatives, containing planar polycyclic systems, represent a large number of antitumor drugs that target DNA.¹ Most of these antiproliferative agents exhibit cytostatic activity through DNA intercalation,² which causes enzymatic blockade and reading errors during the replication process.^{2,3} Intercalators contain a planar chromophore with two to four fused aromatic rings. A positive charge, generally needed for activity,⁴ is usually provided by a quaternized or protonable aromatic nitrogen of the chromophore. The primary nucleic acid intercalation may be further modulated by

binding to other substrates such as topoisomerases⁵ and transition metals.⁶ The redox activity of quinones has also been seen to have a role in the cleavage of DNA mediated by oxygen or sulfur radicals.^{7–9} Actinomycin D (AMD), doxorubicin (doxo), mitoxantrone, and streptonigrin are significant examples of these DNA damaging agents, and their side effects, such as myelosuppression and cardiotoxicity,¹ are related to quinone redox activity.

Recently we described^{10,11} the synthesis and the structure–activity relationships (SARs) of a series of pyridophenoxazinones, which exhibit an antiproliferative activity on a large panel of lymphoblastoid and solid-tumor derived cells at submicromolar concentrations. Molecular modeling studies and NMR investigations suggested that the 5*H*-pyrido[3,2-*a*]phenoxazin-5-one (PPH, **I**; Figure 1), the prototype of the series, intercalates between the 5'-GC-3' base pairs of double-

* To whom correspondence should be addressed. Phone: +39 081 674121. Fax: +39 081 674393. E-mail: bologne@unina.it.

[†] Dipartimento di Chimica Organica e Biochimica, Università di Napoli "Federico II".

[§] Dipartimento di Chimica Farmaceutica e Tossicologica, Università di Napoli "Federico II".

[‡] Università di Cagliari.

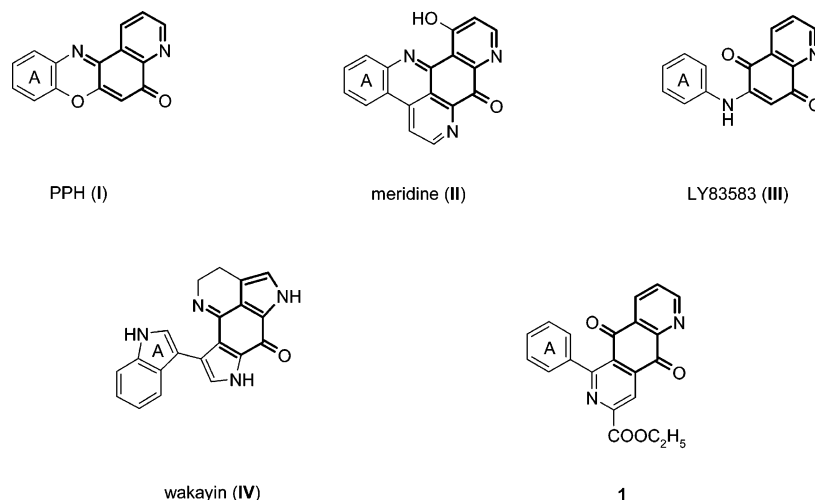


Figure 1. Structures of known anticancer DNA binding agents, with the common quinonic motif highlighted in bold: PPH (I), meridine (II),¹² LY83583 (III),¹³ and wakayin (IV)¹⁴ together with **1** representing the PIQD series.

Chart 1

Comp	R	Comp	R
1	H	8	H
2	NO ₂	9	NO ₂
3	Cl	10	Cl
4	Br	11	Br
5	Me	12	Me
6	OMe	13	OMe
7	N(Me) ₂	14	N(Me) ₂

stranded DNA, involving two strong hydrogen bonds between the hydrogen of the charged pyridine nitrogen and (i) the O4' in the deoxyribose ring of the cytosine C5 residue and (ii) the O5' of the phosphate backbone located between the G4 and C5 residues. Additional stability of the complex arises from π - π stacking interactions between the tetracyclic pyridophenoxazinone system and the aromatic base rings.

In pursuing our research in the field of anticancers, we have investigated a series of 1-aryl-3-ethoxycarbonylpyrido[2,3-*g*]isoquinolin-5,10-diones (PIQDs, **1–7** in Chart 1) that fulfill the requirements for DNA intercalating binding of pyridophenoxazinones.

Molecular modeling studies were performed to verify whether compound **1**, selected as a representative of the PIQD series, possessed the pharmacophoric elements of PPH and of some other antitumor agents that share their common quinonic structural motif (compounds **1** and **I–IV**^{12–14} in Figure 1). This common motif could represent a possible pharmacophore for DNA recognition, a hypothesis that will clearly require more testing for verification. An inspection of the molecular alignment of compounds **I–IV** and **1** shown in Figure 2

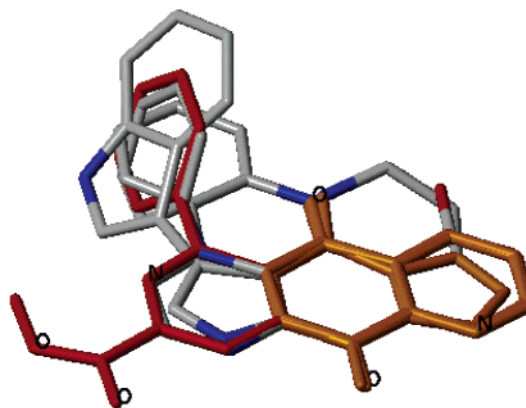
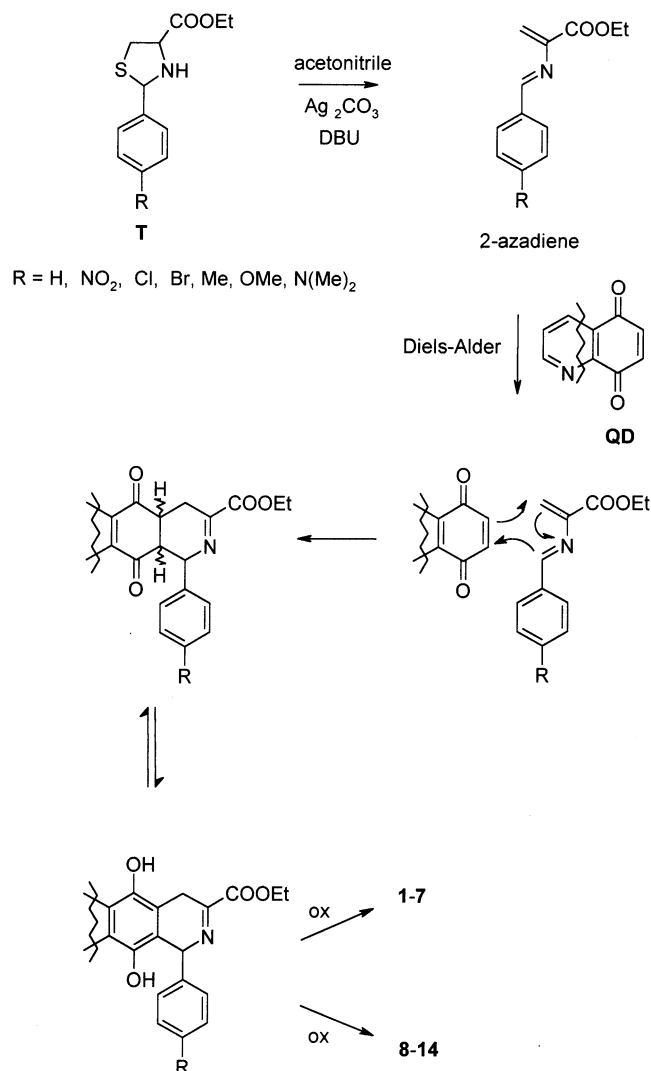


Figure 2. Energy-minimized structures of compounds **I–IV** (by atom) and **1** (red) overlaid on the quinonic substructure shown in orange.

immediately suggests that the phenyl ring at the 6 position of **1** occupies the same position as ring A of PPH and of the other antitumor agents.

Prompted by the above rationale, we synthesized compounds **1–7** and evaluated their antineoplastic

Scheme 1



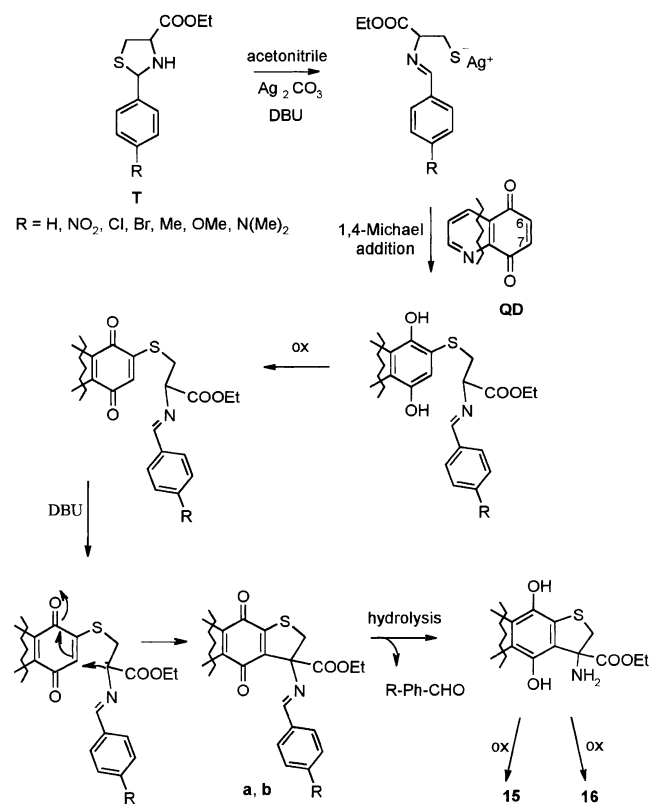
activity against some human cell lines representative of liquid and solid human tumors. The isomeric 1-aryl-3-ethoxycarbonylpyrido[3,2-*g*]isoquinolin-5,10-diones (**8–14**) and the products, the 3-amino-3-ethoxycarbonyldihydrothieno[2,3-*g*]quinolin-4,9-dione (**15**) and 3-amino-3-ethoxycarbonyldihydrothieno[3,2-*g*]quinolin-4,9-dione (**16**), arising from the same synthetic pathway used to obtain **1–7**, were also evaluated for their antiproliferative activity. The noncovalent DNA-binding properties of these compounds were examined using UV–vis, ¹H NMR, and gel-electrophoresis methods.

Results and Discussion

Chemistry. According to the widely reported reactivity of the quinone system toward enophiles in the Diels–Alder reaction and toward nucleophiles in 1,4 Michael addition, the compounds **1–16** seem to be formed by the competitive attack of different species, arising from the demolition of 2-aryl-1,3-thiazolidine ethyl esters (**T** compounds), on quinolin-5,8-dione (QD), through the above-mentioned pathways (Schemes 1 and 2).

T compounds were prepared according to the reported procedure¹⁵ from the L-cysteine ethyl ester and the corresponding benzaldehydes. QD was prepared by hydroxylation followed by oxidation of 5-hydroxyquinoline.¹⁶ A mixture of each **T** (1 mmol) and silver carbonate

Scheme 2



(1 mmol), in anhydrous acetonitrile, at $-20\text{ }^{\circ}\text{C}$ was added to a solution of QD (1 mmol) in anhydrous acetonitrile. After 15 min, 1,8-diazobicyclo[5.4.0]undec-7-ene (DBU, 1 mmol) was added to generate, in situ, the corresponding 2-azadiene. The reaction mixtures, stirred for 2 h at $-20\text{ }^{\circ}\text{C}$ and then kept at room temperature overnight, yielded the corresponding 1-aryl-3-ethoxycarbonylpyrido[2,3-*g*]isoquinolin-5,10-dione (**1–7**) together with the isomeric 1-aryl-3-ethoxycarbonylpyrido[3,2-*g*]isoquinolin-5,10-dione (**8–14**). The dihydrothienoquinolindiones **15** and **16** were obtained as a racemic mixture in all reactions.

Schemes 1 and 2 report a reasonable hypothesis for the formation mechanism of compounds **1–16**. In the basic medium, the breakdown of **T** takes place, yielding a thiolic intermediate and a 2-azadiene.¹⁷ The azadiene attacks the QD double bond via a hetero Diels–Alder reaction,¹⁸ affording two dihydro intermediates that, in turn, yield the corresponding quinone derivatives **1–7** and **8–14** by oxidation (Scheme 1).

As illustrated in Scheme 2, in the 1,4 Michael addition, the thiolate, formed from breakdown of **T**, attacks the 6 and 7 positions of the α,β -unsaturated system of QD, yielding the corresponding diphenol intermediates. After oxidation, an intramolecular cyclization of a carbanion species generates the three-cyclic reduced systems, which yield **15** and **16** according to the position of the heterocyclic nitrogen, by hydrolysis and oxidation. The carbanion species may be formed in the basic medium because of the electron-withdrawing effect of the benzalimine and the carboxy group. The benzalimine derivatives **a** and **b**, isolated and identified in the reaction mixture (not described in this paper), support such a hypothesis for the formation mechanism.

Table 1. Yields of the Reaction between **QD** and **T** Compounds

R	Diels–Alder products		1,4 Michael products	
		yield, %		yield, %
H	1/8	15/10	15/16	18/4
NO ₂	2/9	5/4	15/16	7/2
Cl	3/10	8/8	15/16	8/2
Br	4/11	9/8	15/16	8/4
Me	5/12	20/15	15/16	6/2
OMe	6/13	12/10	15/16	10/8
N(Me) ₂	7/14	22/20	15/16	7/3

Table 1 reports the yields and the product distribution of the reaction between **QD** and the substituted **T** compounds. Electron-donating substituents on the 2-aryl system of **T** increase the yields of the Diels–Alder compounds to the detriment of 1,4 Michael addition products **15** and **16**. This result suggests that electron-donating groups in the para position of the aryl group contribute to the stability of the 2-azadiene formed in situ. The greater amount of **15** compared to **16** is in agreement with both the charge density and orbital coefficient of **QD** at the 6 and 7 positions (for C₆, charge density is 0.0139|e⁻| and LUMO energy is -0.458 91 eV; for C₇, charge density is 0.0076|e⁻| and LUMO energy is 0.324 92 eV),¹⁰ as predicted from the frontier orbital theory.¹⁹

A quantitative interpretation of the reactivity of **QD** vs the 2-azadiene and thiol derivatives using theoretical quantum mechanics computations is currently in progress. The Experimental Section reports general synthetic procedures and characterization of **1–16** on the basis of spectral data and elemental analysis. Structural assignments were accomplished through extensive 2D NMR spectroscopy, HMQC, and HMBC.

Antiproliferative Activity. The antiproliferative activity of the PIQD derivatives **1–7** was evaluated using a panel of nine human cell lines representative of liquid and solid human tumors. The results are shown in Table 2. Data for the anticancer agents PPH, doxo, and AMD are included for comparison.

The median of the IC₅₀ values (the drug concentration inhibiting the mean growth value of cell lines by 50%) shows that the nitro, chloro, and bromo derivatives **2** (median = 0.01 μM), **3** (median = 0.05 μM), and **4** (median = 0.09 μM) were the most cytotoxic compounds, exhibiting an activity comparable with that of PPH (median = 0.04 μM) and doxo (median = 0.03 μM). A particular inhibitory effect was observed on the proliferation of human liquid tumor cells, particularly on acute B-lymphoblastic leukemia (CCRF-SB) and on CD4⁺ T-cells containing an integrated HTLV-1 genome (MT-4), with IC₅₀ values ranging between 0.01 and 0.001 μM. Compound **2** also demonstrated high potency against the splenic B-lymphoblastoid (Wil2-NS, IC₅₀ = 0.001 μM) and against a solid human tumor, skin melanoma (SKMEL-28, IC₅₀ = 0.001 μM). It is interesting to note that the cell lines of solid tumors are more susceptible to the cytotoxic action of **2** than of **3** and **4**. Compounds **2** (median = 0.01 μM), **3** (median = 0.05 μM), and **4** (median = 0.09 μM) showed IC₅₀ values lower than those of **1** (median = 0.50 μM), methyl derivative **5** (median = 0.3 μM), **6** (median = 0.4 μM), and **7** (median = 1.0 μM), suggesting that the presence of electron-withdrawing nitro, chloro, and bromo sub-

stituents in the para position of the pendant phenyl ring **A** (Figure 1) increase cytotoxic activity. As evident from Table 2, the five solid tumor cell lines were substantially less sensitive to compounds **1–7**.

According to the molecular alignment depicted in Figure 2, ring **A** of PIQDs **1–7** occupies the same area as the corresponding benzo-fused ring **A** of PPH, which was found to play a crucial role in the π–π stacking interactions with the base pairs of DNA.¹⁰ Following the previously described intercalation model of PPH,^{10,11} the difference in potency between compounds **2–4** and compounds **1** and **5–7** could be ascribed to electronic effects. In fact, substitution by the electron-withdrawing groups, which pull electrons out of ring **A** and lower the LUMO energy, could improve stacking interactions with purine and pyrimidine bases in the DNA active site. In contrast, the electron-donating methyl, methoxy, and dimethylamino groups, enriching the electron density of ring **A**, could weaken the stacking interactions. This would be in agreement with the activity levels of **1–7**, which decrease according to the nature of the substituent in the order NO₂ < Cl < Br < H < Me < OMe < N(Me)₂.

The other PIQD derivatives **8–14** and the thienoquinolindiones **15** and **16** were also evaluated for their antiproliferative activity against the same panel of human tumor cells (Table 2). Compounds **8–14** were less active than **1–7** with IC₅₀ median values ranging between 0.10 and 2.0 μM, and they exhibited a cytotoxicity about 10- to 100-fold lower than that of **2–4**. However, nitroderivative **9** showed interesting activity and among the tested cell lines; the CCRF-SB cells were particularly sensitive (IC₅₀ = 0.015 μM). By combination of the present findings with the above-mentioned superimposition model, the low cytotoxic activity of **8–14** could be related to the position of the pendant phenyl ring, which, taking the 9 position rather than the 6 position, no longer occupies the same area as the benzo-fused ring **A** of PPH.

The thienoquinolindione **15** (IC₅₀ = 0.08 μM) was 14-fold more active than the isomeric **16** (IC₅₀ = 0.9 μM). It is interesting also to note that **15** was more potent against lymphoblastoid cell lines, having cytotoxic activities comparable to that of PPH and doxo. Among the solid human tumors, prostate carcinoma (DU-145) cells were the most sensitive with an IC₅₀ value of 0.08 μM.

In light of these results, the position of the fused dihydrothieno ring with respect to the quinolinquinonic moiety seems to affect the activity dramatically. This ring, which contains a sulfur atom and both the amino and carbethoxy substituents, may be regarded as a cyclized cysteine fragment. If we assume that **1–16** intercalate to DNA in the same mode as PPH, one may imagine that the amino and carbethoxy groups of **15**, emerging from the drug/DNA complex, interact with the active site of the topoisomerase enzymes. This putative but attractive hypothesis needs further investigation.

To prove whether the ester function might be hydrolyzed during the biological activity tests, compounds **1–16** were transformed in the corresponding acids and tested for their cytotoxicity. No remarkable activity was observed (data not shown), suggesting that the acid function is not involved in the antiproliferative process.

Table 2. Antitumor Activity of **1–16** and PPH Compared to Doxo and AMD

	IC ₅₀ (μM) ^a									
	leukemia/lymphoma				carcinoma					normal cells
	Wil2-NS	CCRF-CEM	CCRF-SB	MT-4	SKMEL-28	MCF-7	SKMES-1	HepG-2	DU-145	CRL-7065
1	0.02	0.20	0.01	0.015	0.8	0.5	0.5	2.0	1.5	nd ^c
2	0.001	0.05	0.002	0.001	0.001	0.08	0.01	0.07	0.01	nd ^c
3	0.01	0.15	0.007	0.006	0.2	0.3	0.05	0.4	0.03	0.04
4	0.02	0.20	0.01	0.01	0.2	0.2	0.09	0.3	0.05	0.05
5	0.03	0.02	0.09	0.3	0.2	1.0	1.0	0.9	1.0	0.07
6	0.09	0.1	0.1	0.4	0.3	1.5	1.6	1.0	1.5	nd ^c
7	1.4	1.2	0.9	0.9	0.9	1.0	1.0	0.9	1.0	nd ^c
8	1.0	0.7	0.6	0.7	0.8	0.3	0.3	1.0	1.0	nd ^c
9	0.03	0.23	0.015	0.01	0.2	0.2	0.08	0.5	0.1	nd ^c
10	2.0	0.8	0.7	0.7	0.8	0.5	0.5	2.0	1.5	0.9
11	2.1	1.3	0.8	0.7	0.9	0.6	0.5	2.3	1.3	1.3
12	2.5	1.0	1.0	1.0	1.3	1.6	1.2	1.9	1.9	nd ^c
13	2.1	1.5	0.9	1.0	1.0	0.9	1.2	2.0	1.5	1.5
14	2.5	2.3	2.2	2.0	1.9	1.6	1.8	2.2	1.9	nd ^c
15	0.06	0.07	0.01	0.02	0.2	0.2	0.1	0.6	0.08	0.09
16	3.1	2.0	0.6	0.5	1.1	0.5	0.9	0.5	1.2	1.7
PPH	0.05	0.01	0.009	0.01	0.21	0.23	0.04	0.05	0.04	0.50
doxo ^b	0.02	0.02	0.03	0.01	0.06	0.05	0.03	0.12	0.03	0.50
AMD ^b	0.0030	0.001	0.002	0.0009	0.002	0.006	0.004	0.010	0.008	0.010

^a Compound concentration required to reduce cell proliferation by 50%, as determined by the MTT method, under conditions allowing untreated controls to undergo at least three consecutive rounds of multiplication. Data represent the mean values of three independent determinations. Abbreviations are the following: Wil2-NS, human splenic B-lymphoblastoid cells; CCRF-CEM, CD4⁺ human acute T-lymphoblastic leukaemia; CCRF-SB, human acute B-lymphoblastic cells; MT-4, CD4⁺ human acute T-lymphoblastic leukemia; SKMEL-28, MCF-7, human breast adenocarcinoma; SKMES-1, human lung squamous carcinoma; HepG-2, human hepatocellular carcinoma; DU-145, human prostate carcinoma; CRL-7065, human foreskin fibroblasts. ^b The doxo and AMD compounds were used as controls. ^c nd = not determined.

Table 3. Effect of **2** on the Proliferation of Wild-Type and Drug-Resistant KB Cells

compd	IC ₅₀ (μM) ^a			
	KB ^{wt} ^b	KB ^{MDR} ^c	KB ^{7D} ^d	KB ^{V20C} ^e
2	0.08 (±0.01)	0.3 (±0.01)	0.4 (±0.01)	0.2 (±0.02)
doxorubicin	0.06 (±0.02)	1.8 (±0.1)	3.0 (±0.2)	0.4 (±0.1)
AMD	0.004 (±0.001)	0.2 (±0.1)	0.2 (±0.1)	0.05 (±0.01)
vincristine	0.004 (±0.001)	1 (±0.2)	0.05 (±0.01)	0.2 (±0.1)
etoposide	0.8 (±0.1)	>20	>20	2.4 (±1.2)

^a Compound concentration required to reduce cell proliferation by 50% as determined by the MTT method under conditions allowing untreated controls to undergo at least three consecutive rounds of multiplication. Data represent mean values (±SD) of three independent determinations. ^b KB human nasopharyngeal carcinoma. ^c KB subclones passaged in the presence of doxorubicin 0.09 μM. ^d KB subclones passaged in the presence of etoposide 7 μM. ^e KB subclones passaged in the presence of vincristine 0.02 μM.

Antiproliferative Activity against Drug-Resistant Tumor Cell Lines. Drug resistance is a relevant therapeutic problem caused by the emergence of tumor cells that confer resistance to a variety of anticancer drugs. The most common mechanisms of drug resistance are related to the overexpression of glycoproteins capable of mediating the efflux of different drugs such as doxorubicin, vincristine, and etoposide and to the altered contents of target enzymes (topoisomerases I and II). Therefore, the inhibitory activity of **2** was evaluated against the following KB subclones (Table 3): (i) KB^{MDR} was obtained by infection of KB^{wt} with a retroviral vector carrying the human *mdr-1* gene and maintained under uninterrupted treatment with doxorubicin. These cells express a membrane glycoprotein (Pgp) responsible for the efflux of many unrelated drugs (multidrug resistance or MDR).^{20,21} (ii) KB^{V20C} was selected under uninterrupted treatment with vincristine. These cells possess an MDR phenotype^{22,23} related to the overexpression of the *mdr-1* gene and mediate the efflux of

doxorubicin, vincristine, and etoposide. (iii) KB^{7D} was selected under uninterrupted treatment with etoposide.²⁴ The resistance is due to overexpression of the *mrp* gene, which codes for a membrane glycoprotein (MRP) capable of mediating the efflux of etoposide, doxorubicin, and vincristine. Interestingly, KB^{V20C}, KB^{MDR}, and KB^{7D} cells were 2.5-fold, 3.7-fold, and 5-fold, respectively, more resistant to **2** relative to the parental KB^{wt} cell line, thus suggesting that this compound is scarcely subject to the pump mediating the efflux of many antitumor drugs.

DNA-Binding Properties. To test the propensity of PIQD compounds to interact with DNA, spectrophotometric measurements and a preliminary ¹H NMR investigation were carried out. The spectroscopic properties of **1** and **15**, selected as representative of series, in the presence and absence of calf thymus DNA were studied by conventional optical spectroscopy. Characterization of this mixture was made by comparing the ultraviolet absorption spectrum of the complex with the spectra of **1** and **15**. The absorption spectra of the free and DNA-bound drugs showed well-defined bathochromic and hypochromic effects. The two absorption bands of **1**, centered at 290 and 360 nm, are red-shifted by about 4 nm, and the hypochromic effect exceeds 30%. The visible absorption maximum of **15**, centered at 418 nm, is red-shifted by about 5 nm, while the hypochromic effect exceeds 28%. These spectral changes suggest the binding of the compounds with the base pairs, while the presence of isosbestic points, at 296 and 370 nm for **1** and at 330 nm for **15**, indicate the existence of a single binding mode with DNA. Similar results were recorded for **2–7**, while no red shift was observed for compounds **8–14** and **16**.

Compound **3** was chosen for the ¹H NMR investigation because it gives easily distinguishable resonance signals and may serve as a reference structure for the

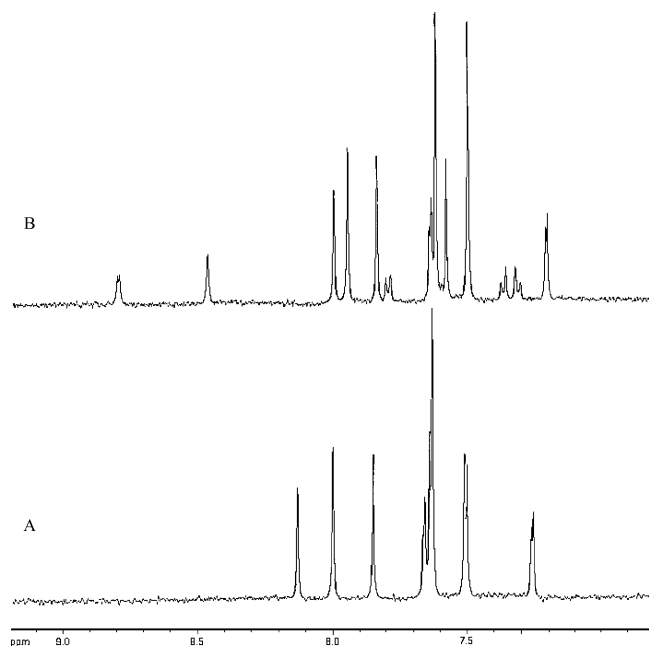


Figure 3. ^1H NMR chemical shift variations of the aromatic region of (A) free octamer $[\text{d}(\text{GAAGCTTC})]_2$ and (B) 1:1 $\mathbf{3}/[\text{d}(\text{GAAGCTTC})]_2$ complex were recorded at 10°C on a 500 MHz spectrometer.

other active compounds. The $[\text{d}(\text{GAAGCTTC})]_2$ octamer, used as the canonical sequence for NMR structural studies of AMD/DNA and PPH/DNA complexes,^{25,10} was expressly synthesized to analyze the $\mathbf{3}/\text{DNA}$ binding.

A titration of the $[\text{d}(\text{GAAGCTTC})]_2$ octamer was carried out in the probe of a Bruker AMX 500 MHz spectrometer at 10°C by addition of small aliquots of $\mathbf{3}$ until a 1:1 ratio of $\mathbf{3}/\text{octamer}$ was reached. The ^1H NMR spectra were recorded with 5 min time intervals between the additions of $\mathbf{3}$ to allow binding equilibration. A comparison of the chemical shifts of the aromatic protons of $\mathbf{3}$ and $[\text{d}(\text{GAAGCTTC})]_2$ with those of the $\mathbf{3}/[\text{d}(\text{GAAGCTTC})]_2$ complex showed that all resonances shifted toward higher fields upon drug addition (Figure 3). All the chemical shifts of $\mathbf{3}$ in the complex are shielded compared to those of the free drug, with the protons H1, H8, and H11 exhibiting shields of 0.60, 0.41, and 0.45 ppm, respectively. The most significant shifts of the octamer are due to the proton H8 of guanine G4 (from 7.62 to 7.59 ppm) and to the protons H6 and H5 of cytosine C5 (from 7.36 to 7.31 ppm and from 5.77 to 5.74 ppm, respectively). Table 4 reports the proton chemical shift assignments of $\mathbf{3}$, G4, and C5 in the $\mathbf{3}/[\text{d}(\text{GAAGCTTC})]_2$ complex and their comparison with both the unbounded ligand and the free octamer. These results provide further evidence that $\mathbf{3}$ binds to DNA and that intercalation occurs, altering the base sequence GC.

Plasmid DNA Unwinding Assay. Since compound $\mathbf{3}$ seems to intercalate at the middle 5'-GC-3' base pairs of the octamer $[\text{d}(\text{GAAGCTTC})]_2$ based on the above-described ^1H NMR experiments, a classic topoisomerase I DNA unwinding assay was employed to determine whether $\mathbf{3}$, binding to DNA, could cause unwinding of a supercoiled plasmid. Figure 4 shows a representative gel electrophoresis of SV40 DNA pre-relaxed with topoisomerase I and then further incubated with $\mathbf{3}$ (0–10 μM) in the presence of topoisomerase I.

Table 4. Proton Chemical Shift Assignments of Unbound $\mathbf{3}$ and of Guanine G4 and Cytosine C5 in the Free Octamer $[\text{d}(\text{GAAGCTTC})]_2$ and Their Comparison with the $\mathbf{3}/[\text{d}(\text{GAAGCTTC})]_2$ Complex

	unbounded $\mathbf{3}$, δ	$\mathbf{3}/[\text{d}(\text{GAAGCTTC})]_2$, δ	$\Delta\delta$
H-1	8.96	8.56	-0.60
H-2	7.88	7.58	-0.30
H-3	9.02	8.71	-0.31
H-6	6.54	6.25	-0.29
H-8	7.51	7.10	-0.41
H-9	7.63	7.42	-0.21
H-10	7.41	7.22	-0.19
H-11	7.88	7.43	-0.45
guanine G4 in $[\text{d}(\text{GAAGCTTC})]_2$			
	$[\text{d}(\text{GAAGCTTC})]_2$, δ	$\mathbf{3}/[\text{d}(\text{GAAGCTTC})]_2$, δ	$\Delta\delta$
H-8	7.65	7.55	-0.10
cytosine C5 in $[\text{d}(\text{GAAGCTTC})]_2$			
	$[\text{d}(\text{GAAGCTTC})]_2$, δ	$\mathbf{3}/[\text{d}(\text{GAAGCTTC})]_2$, δ	$\Delta\delta$
H-5	5.52	5.53	+0.01
H-6	7.36	7.31	-0.05

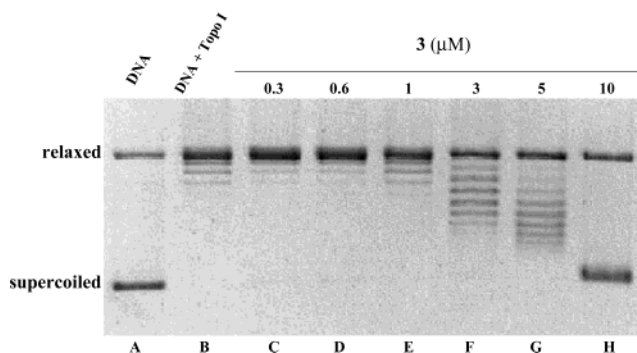


Figure 4. Influence of compound $\mathbf{3}$ on circular DNA topology. Native supercoiled SV40 DNA (lane A) was reacted with an excess of topoisomerase I in the absence of the drug (lane B) or in the presence of increasing concentrations of $\mathbf{3}$ (lanes C–H) for 60 min at 37°C . Reactions were stopped, samples were run on 1% agarose gel in TAE buffer, and DNA topoisomers were visualized after staining with ethidium bromide.

During the reaction, the enzyme relaxes positive supercoils generated by drug-induced duplex unwinding. In this way, topoisomerase I changes DNA linking number in a manner proportional to the magnitude of drug-induced unwinding. Following drug removal by phenol extraction, these altered linking number values result in rewinding of topoisomers from drug-treated samples, whereas control DNA remains relaxed. Under the condition of electrophoresis, the fully relaxed DNA incubated in the absence of drug migrates as slightly positively supercoiled.²⁶ Topoisomer distributions in samples treated with 0.3 and 0.6 μM of $\mathbf{3}$ (lanes C and D, respectively) are consistent with a transition to negative supercoiling that progresses further with increasing concentrations of $\mathbf{3}$, as reflected by the accelerated DNA migration. These characteristic patterns of topoisomer distribution provide the unequivocal evidence for the intercalative mode of $\mathbf{3}$ binding to DNA, as well as of the other derivatives belonging to this series (not shown).

Conclusions

In conclusion, we have described a new series of 1-arylpyridoisoquinolindiones (PIQDs), some of which have levels of cytotoxic activity comparable to that of

doxo against a panel of some liquid and solid tumor cells. The structure-based design was guided by an overlay of compound **1** on some well-known antitumor agents. The IC₅₀ values of these compounds had median values in the range 1.0–0.01 μM, with **2–4** and **15** exhibiting significantly higher in vitro cytotoxic activity. Compound **2** was also evaluated against KB subclones (KB^{MDR}, KB^{7D}, and KB^{V20C}), which overexpress the MDR1/P-glycoprotein drug efflux pump responsible for drug resistance. All the above KB subclones showed scarcely altered sensitivity to the antiproliferative activity of **2**. The noncovalent DNA-binding properties of PIQDs were examined using UV–vis and ¹H NMR spectroscopy experiments. Accordingly, these compounds followed the “classical” pattern observed for intercalation, as provided by the DNA topoisomerase I unwinding assays. Three important features seem to contribute to the cytotoxic activity of these anticancer ligands: (i) the DNA intercalating capability of the three-cyclic quinonic system, typical of this class of compounds, (ii) the position of the pendant phenyl ring, which must occupy the same area of the corresponding benzo-fused ring A of PPH, according to the superimposition model, and (iii) the effect of electron-withdrawing substituents on the phenyl ring, which can contribute to the improvement of the π–π stacking interactions between the ligand and DNA base pairs. The highly active thienoquinolindione **15** (IC₅₀ = 0.08 μM), which can be regarded as a cyclic cysteine derivative, is suspected of interacting with topoisomerases, since both the amino and carbethoxy substituents may be in a favorable position for forming hydrogen bonds with the enzyme/DNA complex.

Whether the cytotoxic activity of the class of compounds that we synthesized is exerted through DNA intercalating binding and/or through other mechanisms is not yet known. Nevertheless, it has been suggested¹ that DNA intercalating anthraquinones can generate disrupting free radical intermediates and alkylating agents. This evidence could account for the cytotoxic activity of **1–16**, which possess a quinone function capable of a one-electron redox reaction. Moreover, these compounds, having an electron-withdrawing carbethoxy substituent on the quinone system, could be more prone structurally to single-electron reduction toward the free radical state. In fact, the capacity of quinones to accept electrons is due to the electron-attracting or -donating substituents that modulate the redox properties responsible for oxidative stress.

From a synthetic point of view, a Diels–Alder reaction and a 1,4 Michael addition originally use the quinoline-5,8-dione and various substituted thiazolidines, enabling **1–16** to be synthesized.

Experimental Section

Chemistry. Melting points were determined by a Kofler apparatus and are uncorrected. The elemental analysis (C, H, and N) of reported compounds agrees with the calculated values and was within ±0.4% of theoretical values. Electron impact (EI) mass spectra were obtained at 70 eV on a ZAB 2F spectrometer. UV spectra were recorded on Perkin-Elmer 550S UV–visible spectrophotometer. The purity of compounds was checked by ascending TLC on Merck's silica gel plates (0.25 mm) with fluorescent baking. NMR measurements (data reported in ppm) were performed on a Bruker AMX-500 spectrometer equipped with a Bruker X-32 computer, using

the UXNMR software package. NMR spectra were measured at 500 MHz (¹H) and 125 MHz (¹³C). The chemical shifts are referenced to ¹³CDCl₃ and CDCl₃ solvent signals at 77.0 and 7.26 ppm, respectively. Standard pulses sequences were employed for magnitude COSY. HMQC and HMBC experiments were optimized for ¹J_{C–H} = 135 Hz and ^{2,3}J_{C–H} = 10 Hz, respectively. Me₄Si was used as an internal reference.

Substituted Phenyl-3-ethoxycarbonylpyridoquinolin-5,10-dione (1–14), 3-Amino-3-ethoxycarbonyldihydrothieno[2,3-g]quinolin-4,9-dione (15), and 3-Amino-3-ethoxycarbonyldihydrothieno[3,2-g]quinolin-4,9-dione (16). General Procedure. A mixture of 2-aryl-1,3-thiazolidine ethyl esters (1 mmol) and silver carbonate (1 mmol), in anhydrous acetonitrile, at –20 °C was added to a solution of quinolin-5,8-dione (1 mmol) in anhydrous acetonitrile. After 15 min, 1,8-diazobicyclo[5.4.0]undec-7-ene (DBU, 1 mmol) was added. The reaction mixture, stirred for 2 h at –20 °C and kept at room temperature overnight, yielded the corresponding 1-aryl-3-ethoxycarbonylpyrido[2,3-g]isoquinolin-5,10-dione (**1–7**) together with the isomeric 1-aryl-3-ethoxycarbonylpyrido[3,2-g]isoquinolin-5,10-dione (**8–14**) separated chromatographically on silica gel plates using a mixture of carbon tetrachloride and ethyl acetate (1:1 v/v) as eluent. The dihydrothienoquinolindiones **15** and **16** were recovered from the reaction as racemic mixture.

1-Phenyl-3-ethoxycarbonylpyrido[2,3-g]isoquinolin-5,10-dione (1): mp, 205–6 °C; UV–vis (CHCl₃) λ_{max} (log ε) nm, 358 (2.6); ¹H NMR (CDCl₃) δ 9.13 (1H, dd, *J* = 4.8, 1.2 Hz), 8.82 (1H, s), 8.64 (1H, dd, *J* = 8.6, 1.2 Hz), 7.79 (1H, dd, *J* = 7.8, 4.8 Hz), 7.59 (2H, d, *J* = 7.0 Hz), 7.47 (3H, d + t, *J* = 7.0 Hz), 4.53 (2H, q, *J* = 7.2 Hz), 1.50 (3H, t, *J* = 7.2 Hz); ¹³C NMR (CDCl₃) δ 181.7 (s, C5), 180.9 (s, C10), 163.6 (s, COO), 162.5 (s, C1), 156.1 (d, C7), 151.8 (s, C3), 149.7 (s, C5a), 141.3 (s, C10a), 138.9 (d, C1'), 135.2 (d, C9), 128.8 (d, C8), 128.7 (s, C9a), 128.5 (2C d, C2'6'), 128.0 (2C d, C3'5'), 126.9 (d, C4a), 126.8 (d, C4'), 119.3 (d, C4), 62.6 (t), 14.2 (q); MS *m/z* 358 (M⁺). Anal. (C₂₁H₁₄N₂O₄) C, H, N.

1-(4-Nitrophenyl)-3-ethoxycarbonylpyrido[2,3-g]isoquinolin-5,10-diones (2): mp, 308–9 °C; UV–vis (CHCl₃) λ_{max} (log ε) nm, 369 (2.8); ¹H NMR (CDCl₃) δ 9.20 (1H, dd, *J* = 4.8, 1.2 Hz), 9.02 (1H, s), 8.52 (1H, dd, *J* = 8.6, 1.2 Hz), 8.37 (2H, d, *J* = 8.6 Hz), 7.81 (1H, dd, *J* = 7.8, 4.8 Hz), 7.69 (2H, d, *J* = 8.6 Hz), 4.56 (2H, q, *J* = 7.2 Hz), 1.48 (3H, t, *J* = 7.2 Hz); ¹³C NMR (CDCl₃) δ 181.5 (s, C5), 180.5 (s, C10), 163.2 (s, COO), 161.8 (s, C1), 156.4 (d, C7), 151.7 (s, C3), 148.2 (s, C5a), 142.4 (s, C10a), 138.9 (s, C1'), 136.7 (d, C4'), 135.4 (d, C9), 132.2 (s, C9a), 130.1 (2C d, C3'5'), 129.0 (d, C8), 123.2 (2C d, C2'6'), 126.1 (s, C4a), 120.7 (d, C4), 62.7 (t), 14.2 (q); MS *m/z* 403 (M⁺). Anal. (C₂₁H₁₃N₃O₆) C, H, N.

1-(4-Chlorophenyl)-3-ethoxycarbonylpyrido[2,3-g]isoquinolin-5,10-diones (3): mp, 208–9 °C; UV–vis (CHCl₃) λ_{max} (log ε) nm, 369 (2.8); ¹H NMR (CDCl₃) δ 9.17 (1H, dd, *J* = 4.8, 1.2 Hz), 8.94 (1H, s), 8.54 (1H, dd, *J* = 8.6, 1.2 Hz), 7.79 (1H, dd, *J* = 7.8, 4.8 Hz), 7.55 (2H, d, *J* = 8.6 Hz), 7.45 (2H, d, *J* = 8.6 Hz), 4.52 (2H, q, *J* = 7.2 Hz), 1.43 (3H, t, *J* = 7.2 Hz); ¹³C NMR (CDCl₃) δ 181.5 (s, C10), 180.8 (s, C5), 163.5 (s, COO), 161.1 (s, C1), 156.2 (d, C7), 151.8 (s, C3), 149.5 (s, C5a), 141.8 (s, C10a), 137.5 (2C d, C2'6'), 135.6 (s, C4'), 135.2 (d, C9), 132.1 (d, C9a), 131.6 (s, C1'), 128.7 (d, C8), 128.4 (2C d, C3'5'), 126.8 (s, C4a), 119.6 (d, C4), 62.5 (t), 14.1 (q); MS *m/z* 392 (M⁺), 394 (M + 2, 32% M⁺). Anal. (C₂₁H₁₃N₂O₄Cl) C, H, N.

1-(4-Bromophenyl)-3-ethoxycarbonylpyrido[2,3-g]isoquinolin-5,10-diones (4): mp, 205–6 °C; UV–vis (CHCl₃) λ_{max} (log ε) nm, 368 (2.8); ¹H NMR (CDCl₃) δ 9.17 (1H, dd, *J* = 4.8, 1.2 Hz), 8.94 (1H, s), 8.54 (1H, dd, *J* = 8.6, 1.2 Hz), 7.79 (1H, dd, *J* = 7.8, 4.8 Hz), 7.58 (2H, d, *J* = 8.6 Hz), 7.34 (2H, d, *J* = 8.6 Hz), 4.52 (2H, q, *J* = 7.2 Hz), 1.43 (3H, t, *J* = 7.2 Hz); ¹³C NMR (CDCl₃) δ 181.5 (s, C10), 180.8 (s, C5), 163.5 (s, COO), 161.1 (s, C1), 156.2 (d, C7), 151.8 (s, C3), 149.5 (s, C5a), 141.8 (s, C10a), 135.2 (d, C9), 132.4 (2C d, C3'5'), 132.1 (d, C9a), 131.6 (s, C1'), 130.5 (2C d, C2'6'), 128.7 (d, C8), 126.8 (s, C4a), 124.6 (s, C4'), 119.6 (d, C4), 62.5 (t), 14.1 (q); MS *m/z* 437 (M⁺), 439 (M + 2, 97% M⁺). Anal. (C₂₁H₁₃N₂O₄Br) C, H, N.

1-(4-Methylphenyl)-3-ethoxycarbonylpyrido[2,3-*g*]isoquinolin-5,10-diones (5): mp, 203–4 °C; UV (CHCl₃) λ_{\max} (log ϵ) nm, 389 (3.3); ¹H NMR (CDCl₃) δ 9.15 (1H, dd, *J* = 4.8, 1.2 Hz), 8.89 (1H, s), 8.53 (1H, dd, *J* = 8.6, 1.2 Hz), 7.76 (1H, dd, *J* = 7.8, 4.8 Hz), 7.46 (2H, d, *J* = 8.6 Hz), 7.30 (2H, d, *J* = 8.6 Hz), 4.53 (2H, q, *J* = 7.2 Hz), 2.42 (3H, s), 1.47 (3H, t, *J* = 7.2 Hz); ¹³C NMR (CDCl₃) δ 181.7 (s, C5), 180.5 (s, C10), 163.7 (s, COO), 162.4 (s, C1), 156.0 (d, C7), 151.5 (s, C3), 149.5 (s, C5a), 141.3 (s, C10a), 139.4 (s, C1'), 136.0 (s, C4'), 135.1 (d, C9), 131.6 (s, C9a), 129.1 (2C d, C2'6'), 128.8 (2C d, C3'5'), 127.9 (d, C8), 125.6 (s, C4a), 118.9 (d, C4), 62.5 (t), 21.4 (q), 14.1 (q); MS *m/z* 372 (M⁺). Anal. (C₂₂H₁₆N₂O₄) C, H, N.

1-(4-Methoxyphenyl)-3-ethoxycarbonylpyrido[2,3-*g*]isoquinolin-5,10-diones (6): mp, 199–200 °C; UV (CHCl₃) λ_{\max} (log ϵ) nm, 391 (3.2); ¹H NMR (CDCl₃) δ 9.15 (1H, dd, *J* = 4.8, 1.2 Hz), 8.89 (1H, s), 8.53 (1H, dd, *J* = 8.6, 1.2 Hz), 7.76 (1H, dd, *J* = 7.8, 4.8 Hz), 7.42 (2H, d, *J* = 8.6 Hz), 7.05 (2H, d, *J* = 8.6 Hz), 4.53 (2H, q, *J* = 7.2 Hz), 3.85 (3H, s), 1.47 (3H, t, *J* = 7.2 Hz); ¹³C NMR (CDCl₃) δ 181.7 (s, C5), 180.5 (s, C10), 163.7 (s, COO), 162.4 (s, C1), 156.0 (d, C7), 151.5 (s, C3), 149.5 (s, C5a), 141.3 (s, C10a), 148.0 (s, C4'), 135.1 (d, C9), 131.6 (s, C9a), 131.4 (s, C1'), 129.1 (2C d, C2'6'), 127.9 (d, C8), 125.6 (s, C4a), 120.8 (2C d, C3'5'), 118.9 (d, C4), 62.5 (t), 54.1 (q), 21.4 (q); MS *m/z* 388 (M⁺). Anal. (C₂₂H₁₆N₂O₅) C, H, N.

1-(4-Dimethylaminophenyl)-3-ethoxycarbonylpyrido[2,3-*g*]isoquinolin-5,10-diones (7): mp, 191–2 °C; UV (CHCl₃) λ_{\max} (log ϵ) nm, 390 (3.2); ¹H NMR (CDCl₃) δ 9.15 (1H, dd, *J* = 4.8, 1.2 Hz), 8.89 (1H, s), 8.53 (1H, dd, *J* = 8.6, 1.2 Hz), 7.76 (1H, dd, *J* = 7.8, 4.8 Hz), 7.15 (2H, d, *J* = 8.6 Hz), 6.80 (2H, d, *J* = 8.6 Hz), 4.53 (2H, q, *J* = 7.2 Hz), 2.85 (6H, s), 1.47 (3H, t, *J* = 7.2 Hz); ¹³C NMR (CDCl₃) δ 181.7 (s, C5), 180.5 (s, C10), 163.7 (s, COO), 162.4 (s, C1), 156.0 (d, C7), 151.5 (s, C3), 149.5 (s, C5a), 149.0 (s, C4'), 141.3 (s, C10a), 135.1 (d, C9), 131.6 (s, C9a), 129.0 (2C d, C2'6'), 127.9 (d, C8), 127.4 (s, C1'), 125.6 (s, C4a), 118.9 (d, C4), 115.8 (2C d, C3'5'), 62.5 (t), 40.3 (2C, q), 21.4 (q); MS *m/z* 401 (M⁺). Anal. (C₂₃H₁₉N₃O₄) C, H, N.

1-Phenyl-3-ethoxycarbonylpyrido[3,2-*g*]isoquinolin-5,10-dione (8): mp, 209–10 °C; UV (CHCl₃) λ_{\max} (log ϵ) nm, 360 (2.9); ¹H NMR (CDCl₃) δ 9.15 (1H, dd, *J* = 4.8, 1.2 Hz), 8.92 (1H, s), 8.52 (1H, dd, *J* = 8.6, 1.2 Hz), 7.77 (1H, dd, *J* = 7.8, 4.8 Hz), 7.54 (2H, d, *J* = 7.0 Hz), 7.51 (2H, t, *J* = 7.2 Hz), 7.47 (1H, t, *J* = 7.0 Hz), 4.53 (2H, q, *J* = 7.2 Hz), 1.47 (3H, t, *J* = 7.2 Hz); ¹³C NMR (CDCl₃) δ 181.6 (s, C10), 180.5 (s, C5), 163.5 (s, COO), 162.2 (s, C1), 155.4 (d, C8), 151.6 (s, C3), 147.7 (s, C9a), 141.7 (s, C10a), 139.4 (s, C1'), 135.8 (d, C6), 131.5 (s, C5a), 129.2 (2C d, C2'6'), 129.0 (2C d, C3'5'), 128.7 (d, C4'), 128.5 (d, C7), 125.5 (s, C4a), 120.0 (d, C4), 62.6 (t), 14.2 (q); MS *m/z* 358 (M⁺). Anal. (C₂₁H₁₄N₂O₄) C, H, N.

1-(4-Nitrophenyl)-3-ethoxycarbonylpyrido[3,2-*g*]isoquinolin-5,10-diones (9): mp, 311–2 °C; UV-vis (CHCl₃) λ_{\max} (log ϵ) nm, 371 (3.0); ¹H NMR (CDCl₃) δ 9.17 (1H, dd, *J* = 4.8, 1.2 Hz), 8.93 (1H, s), 8.68 (1H, dd, *J* = 8.6, 1.2 Hz), 8.34 (2H, d, *J* = 8.6 Hz), 7.82 (1H, dd, *J* = 7.8, 4.8 Hz), 7.73 (2H, d, *J* = 8.6 Hz), 4.56 (2H, q, *J* = 7.2 Hz), 1.48 (3H, t, *J* = 7.2 Hz); ¹³C NMR (CDCl₃) δ 182.1 (s, C10), 181.9 (s, C5), 163.3 (s, COO), 162.5 (s, C1), 155.9 (d, C8), 152.1 (s, C3), 148.9 (s, C9a), 142.9 (s, C10a), 139.3 (s, C1'), 136.5 (d, C4'), 135.9 (d, C6), 130.0 (2C d, C3'5'), 129.5 (d, C5a), 128.4 (d, C7), 125.5 (s, C4a), 123.2 (2C d, C2'6'), 121.3 (d, C4), 63.0 (t), 14.1 (q); MS *m/z* 403 (M⁺). Anal. (C₂₁H₁₃N₃O₆) C, H, N.

1-(4-Chlorophenyl)-3-ethoxycarbonylpyrido[3,2-*g*]isoquinolin-5,10-diones (10): mp, 217–8 °C; UV-vis (CHCl₃) λ_{\max} (log ϵ) nm, 370 (2.9); ¹H NMR (CDCl₃) δ 9.17 (1H, dd, *J* = 4.8, 1.2 Hz), 8.84 (1H, s), 8.63 (1H, dd, *J* = 8.6, 1.2 Hz), 7.82 (1H, dd, *J* = 7.8, 4.8 Hz), 7.50 (2H, d, *J* = 8.6 Hz), 7.47 (2H, d, *J* = 8.6 Hz), 4.55 (2H, q, *J* = 7.2 Hz), 1.46 (3H, t, *J* = 7.2 Hz); ¹³C NMR (CDCl₃) δ 181.6 (s, C10), 180.2 (s, C5), 163.4 (s, COO), 160.9 (s, C1), 155.5 (d, C7), 152.3 (s, C3), 147.7 (s, C9a), 141.3 (s, C10a), 137.1 (2C d, C2'6'), 135.8 (d, C6), 135.6 (s, C4'), 130.4 (s, C1'), 129.4 (s, C5a), 128.6 (d, C7), 128.5 (2C d, C3'5'), 125.7 (s, C4a), 120.3 (d, C4), 62.7 (t), 14.1 (q); MS *m/z* 392 (M⁺), 394 (M + 2, 32% M⁺). Anal. (C₂₁H₁₃N₂O₄Cl) C, H, N.

1-(4-Bromophenyl)-3-ethoxycarbonylpyrido[3,2-*g*]isoquinolin-5,10-diones (11): mp, 209–10 °C; UV-vis (CHCl₃)

λ_{\max} (log ϵ) nm, 368 (2.8); ¹H NMR (CDCl₃) δ 9.15 (1H, dd, *J* = 4.8, 1.2 Hz), 8.86 (1H, s), 8.59 (1H, dd, *J* = 8.6, 1.2 Hz), 7.80 (1H, dd, *J* = 7.8, 4.8 Hz), 7.55 (2H, d, *J* = 8.6 Hz), 7.35 (2H, d, *J* = 8.6 Hz), 4.52 (2H, q, *J* = 7.2 Hz), 1.43 (3H, t, *J* = 7.2 Hz); ¹³C NMR (CDCl₃) δ 181.5 (s, C10), 180.8 (s, C5), 163.5 (s, COO), 161.9 (s, C1), 157.2 (d, C7), 151.8 (s, C3), 149.5 (s, C5a), 141.8 (s, C10a), 135.2 (d, C9), 132.2 (2C d, C3'5'), 132.1 (d, C9a), 132.0 (s, C1'), 130.5 (2C d, C2'6'), 128.7 (d, C8), 126.8 (s, C4a), 124.6 (s, C4'), 119.6 (d, C4), 62.5 (t), 14.1 (q); MS *m/z* 437 (M⁺), 439 (M + 2, 97% M⁺). Anal. (C₂₁H₁₃N₂O₄Br) C, H, N.

1-(4-Methylphenyl)-3-ethoxycarbonylpyrido[3,2-*g*]isoquinolin-5,10-diones (12): mp, 208–9 °C; UV-vis (CHCl₃) λ_{\max} (log ϵ) nm, 391 (3.5); ¹H NMR (CDCl₃) δ 9.16 (1H, dd, *J* = 4.8, 1.2 Hz), 8.78 (1H, s), 8.64 (1H, dd, *J* = 8.6, 1.2 Hz), 7.80 (1H, dd, *J* = 7.8, 4.8 Hz), 7.51 (2H, d, *J* = 8.6 Hz), 7.27 (2H, d, *J* = 8.6 Hz), 4.53 (2H, q, *J* = 7.2 Hz), 2.45 (3H, s), 1.46 (3H, t, *J* = 7.2 Hz); ¹³C NMR (CDCl₃) δ 181.8 (s, C10), 181.1 (s, C5), 163.6 (s, COO), 162.3 (s, C1), 155.3 (d, C8), 151.8 (s, C3), 147.7 (s, C9a), 141.7 (s, C10a), 139.5 (s, C1'), 136.5 (s, C4'), 136.5 (d, C6), 129.9 (s, C5a), 129.3 (2C d, C2'6'), 128.9 (2C d, C3'5'), 128.7 (d, C7), 126.9 (s, C4a), 119.7 (d, C4), 62.5 (t), 21.3 (q), 14.2 (q); MS *m/z* 372 (M⁺). Anal. (C₂₂H₁₆N₂O₄) C, H, N.

1-(4-Methoxyphenyl)-3-ethoxycarbonylpyrido[3,2-*g*]isoquinolin-5,10-diones (13): mp, 205–6 °C; UV (CHCl₃) λ_{\max} (log ϵ) nm, 395 (3.1); ¹H NMR (CDCl₃) δ 9.14 (1H, dd, *J* = 4.8, 1.2 Hz), 8.87 (1H, s), 8.55 (1H, dd, *J* = 8.6, 1.2 Hz), 7.75 (1H, dd, *J* = 7.8, 4.8 Hz), 7.41 (2H, d, *J* = 8.6 Hz), 7.07 (2H, d, *J* = 8.6 Hz), 4.53 (2H, q, *J* = 7.2 Hz), 3.85 (3H, s), 1.47 (3H, t, *J* = 7.2 Hz); ¹³C NMR (CDCl₃) δ 181.6 (s, C5), 180.5 (s, C10), 163.9 (s, COO), 162.3 (s, C1), 156.2 (d, C7), 151.5 (s, C3), 149.0 (s, C5a), 140.8 (s, C10a), 148.0 (s, C4'), 135.1 (d, C9), 131.6 (s, C9a), 132.4 (s, C1'), 129.8 (2C d, C2'6'), 127.9 (d, C8), 125.6 (s, C4a), 121.5 (2C d, C3'5'), 118.9 (d, C4), 62.5 (t), 54.3 (q), 21.4 (q); MS *m/z* 388 (M⁺). Anal. (C₂₂H₁₆N₂O₅) C, H, N.

1-(4-Dimethylaminophenyl)-3-ethoxycarbonylpyrido[3,2-*g*]isoquinolin-5,10-diones (14): mp, 200–1 °C; UV (CHCl₃) λ_{\max} (log ϵ) nm, 388 (3.2); ¹H NMR (CDCl₃) δ 9.11 (1H, dd, *J* = 4.8, 1.2 Hz), 8.87 (1H, s), 8.58 (1H, dd, *J* = 8.6, 1.2 Hz), 7.72 (1H, dd, *J* = 7.8, 4.8 Hz), 7.14 (2H, d, *J* = 8.6 Hz), 6.82 (2H, d, *J* = 8.6 Hz), 4.53 (2H, q, *J* = 7.2 Hz), 2.84 (6H, s), 1.47 (3H, t, *J* = 7.2 Hz); ¹³C NMR (CDCl₃) δ 181.6 (s, C5), 180.0 (s, C10), 163.7 (s, COO), 162.4 (s, C1), 156.0 (d, C7), 151.5 (s, C3), 149.5 (s, C5a), 149.0 (s, C4'), 141.3 (s, C10a), 135.1 (d, C9), 131.6 (s, C9a), 129.0 (2C d, C2'6'), 127.9 (d, C8), 127.4 (s, C1'), 125.6 (s, C4a), 118.9 (d, C4), 115.8 (2C d, C3'5'), 62.5 (t), 40.3 (2C, q), 21.4 (q); MS *m/z* 401 (M⁺). Anal. (C₂₃H₁₉N₃O₄) C, H, N.

3-Amino-3-ethoxycarbonyldihydrothieno[2,3-*g*]quinolin-4,9-dione (15): mp > 200 °C dec; UV (CHCl₃) λ_{\max} (log ϵ) nm, 418 (3.6); ¹H NMR (CDCl₃) δ 9.01 (1H, dd, *J* = 6.3, 1.6 Hz), 8.40 (1H, dd, *J* = 8.2, 1.6 Hz), 7.64 (2H, d, *J* = 8.2 Hz), 4.27 (2H, q, *J* = 7.2 Hz), 3.87 (1H, d, *J* = 12.4 Hz), 3.34 (1H, d, *J* = 12.4 Hz), 1.27 (3H, t, *J* = 7.2 Hz); ¹³C NMR (CDCl₃) δ 180.7 (s, C5), 179.9 (s, C9), 172.5 (s, COO), 154.9 (s, C5a), 154.3 (d, C2), 146.7 (s, C9a), 142.0 (s, C8a), 139.1 (s, C4a), 136.7 (d, C4), 128.2 (d, C3), 73.3 (s, C8), 62.6 (t), 42.4 (t, C7), 14.0 (q); MS *m/z* 304 (M⁺), 306 (M + 2, 11% M⁺), 308 (M + 4, 4% M⁺). Anal. (C₁₄H₁₂N₂O₄S) C, H, N.

3-Amino-3-ethoxycarbonyldihydrothieno[3,2-*g*]quinolin-4,9-dione (16): mp > 200 °C dec; UV (CHCl₃) λ_{\max} (log ϵ) nm, 413 (3.2); ¹H NMR (CDCl₃) δ 9.0 (1H, dd, *J* = 6.3, 1.6 Hz), 8.38 (1H, dd, *J* = 8.2, 1.6 Hz), 7.62 (2H, d, *J* = 8.2 Hz), 4.27 (2H, q, *J* = 7.2 Hz), 3.85 (1H, d, *J* = 12.4 Hz), 3.36 (1H, d, *J* = 12.4 Hz), 1.27 (3H, t, *J* = 7.2 Hz); ¹³C NMR (CDCl₃) δ 180.1 (s, C9), 180.0 (s, C5), 171.9 (s, COO), 155.5 (d, C2), 154.7 (s, C8a), 146.8 (s, C9a), 142.2 (s, C5a), 138.9 (s, C4a), 135.8 (d, C4), 128.5 (d, C3), 72.0 (s, C6), 62.5 (t), 43.1 (t, C7), 14.1 (q); MS *m/z* 304 (M⁺), 306 (M + 2, 11% M⁺), 308 (M + 4, 4% M⁺). Anal. (C₁₄H₁₂N₂O₄S) C, H, N.

Biology. Test compounds were dissolved in DMSO at an initial concentration of 200 μ M and then were serially diluted in culture medium.

Cells. Cell lines were from American Type Culture Collection (ATCC). Leukemia- and lymphoma-derived cells were grown in RPMI 1640 containing 10% fetal calf serum (FCS), 100 U/mL penicillin G, and 100 μ g/mL streptomycin. Solid-tumor derived cells were grown in their specific media supplemented with 10% FCS and antibiotics. The nasopharyngeal carcinoma KB cell line and the resistant mutant subclones KB^{MDR}, KB^{V20C}, KB^{7D} were a generous gift of Prof. Y. C. Cheng, Yale University (New Haven, CT). All resistant KB cell lines were maintained in growth medium supplemented with 0.09 μ M doxorubicin for KB^{MDR}, 0.02 μ M vincristine for KB^{V20C}, and 7 μ M etoposide for KB^{7D}. Cell cultures were incubated at 37 °C in a humidified 5% CO₂ atmosphere. Cell cultures were checked periodically for the absence of mycoplasma contamination by the Hoechst staining method.

Antiproliferative Assays. Exponentially growing leukemia and lymphoma cells were resuspended at a density of 1×10^5 cells/mL in RPMI containing serial dilutions of the test drugs. Cell viability was determined after 96 h at 37 °C by the 3-(4,5-dimethylthiazol-2-yl)-2,5-diphenyltetrazolium bromide (MTT) method. Activity against solid tumor derived cells was evaluated in exponentially growing cultures seeded at 5×10^4 cells/mL and allowed to adhere for 16 h to culture plates before addition of the drugs. Cell viability was determined by the MTT method 4 days later.

Linear Regression Analysis. Tumor cell growth at each drug concentration was expressed as a percentage of untreated controls, and the concentration resulting in 50% (IC₅₀) growth inhibition was determined by linear regression analysis.

DNA Unwinding Assays. The pyridoisoquinolindione-induced DNA unwinding was examined using topoisomerase I assay.²⁶ Supercoiled SV40 DNA (0.4 μ g) was incubated with 5 U of topoisomerase I (Life Technologies Inc.) in 30 μ L of Topo I reaction buffer. After 5 min at 37 °C, a compound to be tested was added and the incubation continued for 60 min. Reactions were stopped by addition of dodecyl sulfate (SDS) and proteinase K (final concentrations of 1% and 0.5 mg mL⁻¹, respectively). After an additional 15 min at 37 °C, the samples were extracted with a phenol/chloroform/isoamyl alcohol mixture (25:24:1 v/v) and electrophoresed overnight at 1 V cm⁻¹ in 1% agarose gel using TAE buffer (40 mM Tris-acetate, 10 mM EDTA, pH 8.0). DNA bands were visualized with ethidium bromide (0.5 μ g mL⁻¹) and photographed under UV

Spectrophotometry. Molar extinction coefficients at the wavelength of maximum absorption in the visible spectrum were determined for **1** free in solution and for **1** bound to calf thymus DNA (Sigma Chemical Company, St. Louis, MO). Measurements were made in 0.1 SHE buffer [2 mM 4-(2-hydroxyethyl)-1-piperazineethanesulfonic acid, 10 mM EDTA, and 99.4 mM NaCl (pH 7.0)]/DMSO (1:1 v/v) at 25 °C. Spectra were recorded at a drug concentration of 0.05 mM in the presence of 1 mM calf thymus DNA.

Molecular Modeling. All molecular modeling was conducted using the software package SYBYL²⁷ running on a Silicon Graphics Octane2 workstation. Input coordinates of compounds **1** and **I–IV** were built according to SYBYL standard bond lengths and valence angles. Geometry optimizations were performed with the semiempirical quantum mechanics methods AM1,²⁸ available in the MOPAC program²⁹ (keywords: PREC, GNORM = 0.01, EF). Molecules were superimposed by minimization of the root-mean-square distance between selected atom pairs using the SYBYL/FIT command. Compound **1**, selected as being representative of the PIQD series, was fitted on **I–IV** about the following points: (i) the common quinolinquinonic moiety highlighted in bold face in Figure 1 and (ii) the centroid of the ring A.

Acknowledgment. The authors thank the Centro Interdipartimentale di Metodologie Chimico-Fisiche and the Centro Interdipartimentale di Analisi Strumentale dell'Università di Napoli "Federico II". This work was supported by a grant from Ministero dell'Università e della Ricerca Scientifica.

References

- Chabner, B. A.; Allegra, C. J.; Curt, G. A.; Calabresi, P.; Antineoplastic Agents. In *Goodman and Gilman's The Pharmacological Basis of Therapeutics*, 9th ed.; Hardman, J. G., Limbird, L. E., Molinoff, P. B., Ruddon, R. W., Gilman, A. G., Eds.; McGraw-Hill: New York, 1996; pp 1233–1287.
- Wakelin, L. P. G.; Waring, M. J. DNA Intercalating Agents. In *Comprehensive Medicinal Chemistry*; Sammes, P. G., Ed.; Pergamon Press: Oxford, U.K., 1990; Vol. 2, pp 703–724.
- Saenger, W. *Principles of Nucleic Acid Structures*; Springer: New York, 1983.
- Waring, M. J. Variation of the Supercoils in Closed Circular DNA by Binding of Antibiotics and Drugs. Evidence for Molecular Models Involving Intercalation. *J. Mol. Biol.* **1970**, *54*, 247–279.
- Tewey, K. M.; Chen, G. L.; Nelson, E. M.; Liu, L. F. Intercalative Anticancer Drugs Interfere with the Breakage–Reunion Reaction of Mammalian DNA Topoisomerase II. *J. Biol. Chem.* **1984**, *259*, 9182–9187.
- Marcazzan, M.; Gatto, B.; Sissi, C.; Fagotto, G.; Capranico, G.; Palumbo, M. Further Insight into the Zn²⁺-Mediated Binding of Streptogrin to DNA. *Farmaco* **1998**, *53*, 645–649.
- Bachur, N. R.; Gordon, S. L.; Gee, M. V. A General Mechanism for Microsomal Activation of Quinone Anticancer Agents to Free Radicals. *Cancer Res.* **1978**, *38*, 1745–1750.
- Beall, H. D.; Murphy, A. M.; Siegel, D.; Hargreaves, R. H. J.; Butler, J. D. NAD(P)H:Quinone as a Target for Bioreductive Antitumor Quinones: Quinone Cytotoxicity and Selectivity in Human Lung and Breast Cancer Cell Lines. *Mol. Pharmacol.* **1995**, *48*, 499–504.
- Matsumoto, S. S.; Sidford, M. H.; Holden, J. A.; Barrows, L. R.; Copp, B. R. Mechanism of Action Studies of Cytotoxic Marine Alkaloids: Ascidiemin Exhibits Thiol-Dependent Oxidative DNA Cleavage. *Tetrahedron Lett.* **2000**, *41*, 1667–1670.
- Bolognese, A.; Correale, G.; Manfra, M.; Lavecchia, A.; Mazzoni, O.; Novellino, E.; Barone, V.; La Colla, P.; Loddio, R.; Murgioni, C.; Pani, A.; Serra, I.; Setzu, G. Antitumor Agents. 1. Synthesis, Biological Evaluation and Molecular Modeling of 5*H*-Pyrido[3,2-*a*]phenoxazin-5-one, a New Compound with Potent Antiproliferative Activity. *J. Med. Chem.* **2002**, *45*, 5205–5216.
- Bolognese, A.; Correale, G.; Manfra, M.; Lavecchia, A.; Mazzoni, O.; Novellino, E.; Barone, V.; La Colla, P.; Loddio, R. Antitumor Agents. 2. Synthesis, Structure–Activity Relationships and Biological Evaluation of Substituted 5*H*-Pyridophenoxazin-5-ones with Potent Antiproliferative Activity. *J. Med. Chem.* **2002**, *45*, 5217–5223.
- Delfourne, E.; Darro, F.; Bontemps-Subielos, N.; Decaestecker, C.; Bastide, J.; Frydman, A.; Kiss, R. Synthesis and Characterization of the Antitumor Activities of Analogues of Meridine, a Marine Pyridoacridine Alkaloid. *J. Med. Chem.* **2001**, *44*, 3275–3282.
- Lee, Y. S.; Wurster, R. D. Mechanism of Potentiation of LY83583-Induced Growth Inhibition by Sodium Nitroprusside in Human Brain Tumor Cells. *Cancer Chemother. Pharmacol.* **1995**, *36*, 341–344.
- Kokoshka, J. M.; Capson, T. L.; Holden, J. A.; Ireland, C. M.; Barrows, L. R. Differences in the Topoisomerase I Cleavage Complexes Formed by Camptothecin and Wakayin, a DNA-Intercalating Marine Natural Product. *Anti-Cancer Drug Des.* **1996**, *7*, 758–765.
- Yasuda, M.; Boger, D. L. Streptonigrin and Lavendamycin Partial Structures. Preparation of 7-Amino-2-(2'-pyridyl)quinoline-5,8-quinone-6'-carboxylic Acid: A Probe for the Minimum, Potent Pharmacophore of the Naturally Occurring Antitumor-Antibiotics. *J. Heterocycl. Chem.* **1987**, *24*, 1253–1260.
- Barret, R.; Daudon, M. Oxidation of Phenols to Quinones by Bis-(trifluoroacetoxy)iodobenzene. *Tetrahedron Lett.* **1990**, *31*, 4871–4872.
- Öhler, E.; Schmidt, U. Schiffche Basen von Dehydroaminessäuren aus 2-Aryl-4-thiazolidincarbonsäuren. Erste Synthese eines *N*-Aryliden-dehydroalaninesters. *Chem. Ber.* **1979**, *112*, 107–115.
- Gilchrist, T. L.; Gonsalves, A. M. A. R.; Pinho e Melo, T. M. V. Diels–Alder Reactions of 2-Azadienes Derived from Cysteine and Serine Methyl Esters and Aldehydes. *Tetrahedron* **1994**, *50*, 13709–13724.
- Fleming, I. *Frontier Orbitals and Organic Chemical Reactions*; John Wiley & Sons: Chichester, U.K., 1976.
- Endicott, J. A.; Ling, V. The Biochemistry of P-Glycoprotein-Mediated Multidrug Resistance. *Annu. Rev. Biochem.* **1989**, *58*, 137–171.
- Twentyman, P. R. Multidrug Resistance Strategy for Circumvention. *Drug News Perspect.* **1993**, *6*, 647–654.
- Pastan, I.; Gottesman, M. M.; Ueda, K.; Lovelace, E.; Rutherford, A. V.; Willingham, M. C. A Retrovirus Carrying an MDR1 cDNA Confers Multidrug Resistance and Polarized Expression of P-Glycoprotein. *Proc. Natl. Acad. Sci. U.S.A.* **1988**, *85*, 4486–4490.

- (23) Chen, H. X.; Bamberger, U.; Heckel, A.; Guo, X.; Cheng, Y. C. BIBW 22, a Dipyridamole Analogue, Acts as Bifunctional Modulator on Tumor Cells by Influencing Both P-Glycoprotein and Nucleoside Transport. *Cancer Res.* **1993**, *53*, 1974–1977.
- (24) Gaj, C. L.; Anyanwutaku, I.; Chang, Y. H.; Cheng, Y. C. Decreased Drug Accumulation without Increased Drug Efflux in a Novel MRP-Overexpressing Multidrug-Resistant Cell Line. *Biochem. Pharmacol.* **1998**, *55*, 1199–2110.
- (25) Takusagawa, F.; Takusagawa, K. T.; Carlson, R. G.; Weaver, R. F. Selectivity of F8-Actinomycin D for RNA:DNA Hybrids and Its Anti-leukemia Activity. *Bioorg. Med. Chem.* **1997**, *5*, 1197–207.
- (26) Pommier, Y.; Covey, J. M.; Kerrigan, D.; Markovits, J.; Pham, R. DNA unwinding and inhibition of mouse leukemia L1210 DNA topoisomerase I by intercalators. *Nucleic Acids Res.* **1987**, *15*, 6713–6731.
- (27) SYBYL Molecular Modelling System, version 6.8; Tripos Inc.: St. Louis, MO.
- (28) Dewar, M. J. S.; Zoebisch, E. G.; Healy, E. F.; Stewart, J. J. P. AM1: A New General Purpose Mechanical Molecular Model. *J. Am. Chem. Soc.* **1985**, *107*, 3902–3909.
- (29) MOPAC (version 6.0) is available from Quantum Chemistry Program Exchange, No. 455.

JM030918B